12-2014

A New Approach to Optimization of Dynamic Reactive Power Sources Addressing FIDVR Issues

Weihong Huang
University of Tennessee - Knoxville, whuang12@vols.utk.edu

To the Graduate Council:

I am submitting herewith a thesis written by Weihong Huang entitled "A New Approach to Optimization of Dynamic Reactive Power Sources Addressing FIDVR Issues." I have examined the final electronic copy of this thesis for form and content and recommend that it be accepted in partial fulfillment of the requirements for the degree of Master of Science, with a major in Electrical Engineering.

Kai Sun, Major Professor

We have read this thesis and recommend its acceptance:

Fangxing Li, Yan Xu

Accepted for the Council:
Carolyn R. Hodges

Vice Provost and Dean of the Graduate School

(Original signatures are on file with official student records.)

A New Approach to Optimization of Dynamic Reactive Power Sources Addressing FIDVR Issues

A Thesis Presented for the

Master of Science

Degree

The University of Tennessee, Knoxville

Weihong Huang

December 2014

Acknowledgements

I would like to thank first and foremost to my supervisor Dr. Kai Sun, for his kind guidance, help and support on my research work. I really appreciate the opportunity he provided for me to be able to study in UTK. During the past one and a half years, his generous suggestions and brilliant ideas help me gain a lot on the field of power system. He is also willing to share with me his career stories, which is not only useful for my research work, but also beneficial to my personal life.

I also want to show my gratitude to my other committee members. Dr. Fangxing "Fran" Li's different courses in power system give me a broad view on this area, and help me build a solid foundation for my research. Dr. Yan Xu also gives me a lot of help on my project. Her expertise in power system and power electronics helps me to improve the project in this thesis.

I would also like to thank Oak Ridge National Laboratory (ORNL). This thesis's project is supported by ORNL under Management and Optimization of Vars for Future Transmission Infrastructure with High Penetration of Renewable Generation (MOVARTI) project.

I would like to thank all my fellow students in CURENT for their help on the research work, and I will cherish our friendship for my whole life. They are Mr. Fengkai Hu, Dr. Junjian Qi, Mr. Bin Wang, Mr. Nan Duan, Mr. Denis Osipov, Mr. Yongli Zhu, Mr. Wenyun Ju, Mr. Rui Yao, Mr. Dongsheng Cai and Miss Feifei Bai.

Last but not least, I would like to thank my parents. Their endless love and encourage give me the strong support for my study and life abroad. I really want to thank my husband Zheyu Zhang. Your encouragement and support are the inner motive for me to pursue my dream here.

Abstract

Dynamic reactive power (var) sources, e.g. SVCs and STATCOMs, can effectively mitigate fault-induced delayed voltage recovery (FIDVR) issues or even voltage collapse. However, their optimal allocation in a power grid is a complicated nonlinear optimization problem since the post-fault voltage trajectories have to be solved to check constraints on voltage responses. Thus, solvers of both nonlinear optimization and power system differential and algebraic equations (DAEs) are required.

Currently, most of existing methods merely achieve dynamic optimization locally with great dependence on the initial operation point. Also, complicated algorithm and time consuming are obstacles for the practical implementation.

This thesis proposes a new approach to optimize the sizes of dynamic var sources at candidate locations by efficiently interfacing a heuristic linear programming based searching algorithm with power system simulation software. Within several iterative search steps, the optimal size of dynamic var can be achieved. In order to verify the result obtained from the proposed approach, Voronoi diagram is applied to tackle the feasible solution area, and then to demonstrate the result of heuristic linear programming is the global optimal.

Case studies on a 9-bus system and the IEEE 39-bus system have benchmarked the new approach with an existing representative approach and demonstrated that the new approach can quickly converge to an optimal solution. Voronoi diagram is implemented

to tackle non-convex feasible solution area of both cases and it shows that the result is global optimal.

Index Terms—dynamic var support; FIDVR; linear programming, nonlinear optimization; voltage recovery; Voronoi diagram

Table of Contents

List of Tables

List of Figures

Chapter 1 Introduction

This chapter starts with an introduction to the background of voltage security issues and Voronoi diagram. Main characteristics and detrimental effect of voltage instability and the state-of-art research activities are reviewed. Also, the basic idea and development of Voronoi diagram are introduced. Afterwards, the objectives of the thesis are discussed, and the structure and organization of the thesis are presented.

1.1 Research background

1.1.1 Voltage security issues

For decades, angle stability problems had been extensively investigated in power system stability studies since it was considered to be responsible for most instability phenomena including voltage related events [1]. However, the change of the power system structure and operation, have caused the voltage instability issue to be an independent phenomenon.

Voltage security issues in a power grid have attracted more attention due to ever-growing electricity demands. Other than depressed voltage profiles, utilities also have increasing concerns with dynamic voltage security issues, especially fault-induced delayed voltage recovery (FIDVR) issues at load buses and even fast voltage collapse following cascading events, because of the increasing dynamic fast-responding loads, such as the air conditions with high-efficiency low-inertia motors. The dynamic behavior of motor loads, such as decelerating and stalling in the event of voltage sags, as well as a huge amount of reactive power consumed by the stalled motors delay the voltage

recovery. The dynamic and fast characteristics of short-term voltage instability demands fast and sufficient reactive power injection. Therefore, the management of dynamic var sources especially their optimal location and size, becomes an emerging research topic.

Several previous reported studies have investigated the optimal allocation of dynamic var sources [2]-[7]. Reference [2] studies the placement of SVCs by using post-contingency trajectory sensitivity analysis. The study is focused on examining the impact of a fault at bulk transmission level in the system during peak load condition. The power system components were modeled in details, including both static and dynamic loads at key distribution feeders, over excitation limiters, switchable shunts, STATCOM, and static var compensator. The concept of trajectory sensitivity index was proposed to identify the location for dynamic var support for the mitigation of the short-term voltage instability problem caused by large disturbances.

In [3], the sizes and locations of var sources were determined by means of optimal power flow (OPF), and verified by P-V and Q-V analysis. The OPF typically provided the optimal locations and sizes for VAR injection devices that satisfied the given constraints. However, the dynamic var amount obtained may not be optimal since it uses a steady state approach to find the initial amount and only refines the amount by simulating in time domain.

In [4], OPF was also applied to determine a right mix of static and dynamic var supports. As part of the static analysis, power flow and P-V analysis were performed to investigate thermal problems and determine load serving capability. Dynamic analysis

was used to study fast voltage collapse phenomenon and perform load sensitivity studies. As a final verification, the mid-term time-domain simulation is performed for refining the solution.

In [5], a technique titled “the time continuation method” was applied to find the locations and amounts of dynamic var sources, coupling with a quadratic model of the electric power system, including generators, voltage regulators, and induction motors. However, this method still cannot capture the full dynamics of the system because it used only a quadratic steady state model of generators and loads.

In [6] and [7], the dynamic var allocation problem was formulated as a mixed integer nonlinear programing problem. The var locations and an initial guess on var sizes were respectively from a trajectory sensitivity study and a linear programming (LP) algorithm [2], and then the final solutionwas obtained by interfacing an optimization tool with power system time-domain simulation software to optimize the required var amounts for each time step of the post-contingency trajectories [6].

1.1.2 Voronoi diagram

Voronoi diagram is one of the most useful data structures in computational geometry, which was widely applied to diverse fields of science and engineering such as finite element meshing, image processing, architectural design, physical simulation, visualization. In this thesis, Voronoi diagrams were adopted in the visualization of contour map.

[8] gives whole perspectives of Voronoi diagram mainly in five perspectives including structure, computing, line segments, farthest point and a few historical remarks. Some properties of the Voronoi diagram has been proved as well. For example, if one connects all the pairs of sites of which Voronoi cells are adjacent, the resulting set of segments forms a triangulation of the point set, called the Delaunay triangulation. This triangulation with several excellent properties, is one of the approximation methods widely used in variety areas.

In [9], a simple but efficient approach for computing the localized restricted Voronoi diagrams on mesh surfaces was presented. Restricted Voronoi diagram can contain Voronoi regions that consist of multiple disjoint surface patches. Also, localized restricted Voronoi diagrams is a useful extension to improve several existing mesh-processing techniques, most importantly surface remeshing with a low number of vertices.

In [10], a Voronoi diagram based blending method of local response surfaces was proposed to accomplish global fidelity in function approximation for engineering designing optimization. The method compromised the tradeoffs between local and global properties in function approximation through adaptive cumulation of sample points based on Voronoi diagram geometric information on their distribution. Additionally, the approximation was gradually refined in ever smaller Voronoi regions with quadratic polynomial expression.

1.2 Objective

This thesis aims at implementing a fast algorithm to find the optimal dynamic var location and size. The challenges come from the complexity of the optimal allocation of dynamic var sources, since the problem itself is a nonlinear optimization problem and its constraints check requires the information of post-fault power system trajectories. Thus both a nonlinear optimization solver and a power system DAE solver are required and they should be systematically integrated or interfaced for an efficient algorithm to solve the problem. Most of the existing methods either solve a simplified problem for an approximate solution or suffer computational burdens for large-scale power systems if two solvers are interacted frequently. Furthermore, the result of existing method may not be global optimal which may rely on the initial value.

The approach proposed in this thesis solves the optimal dynamic var allocation problem by systematically interfacing power system time-domain simulation software with a LP based heuristic search algorithm. Compared to the approach in [7], it takes a small number of iterative steps to quickly converge to an optimal solution, and at each step, the LP can effectively identify the searching direction for reducing the cost function toward an optimum. Thus, the new approach has moderate computation burdens. The proposed approach is demonstrated on the WECC 9-bus system and the IEEE 39-bus system [11]. In order to verify the result of the Linear programming based Heuristic search algorithm is global optimal, Voronoi diagram is applied to establish contour map of the feasible solution area.

1.3 Organization

The chapters of this thesis are organized as follows:

Chapter 2 introduces the WECC/NERC transient voltage dip and overshoot standards follows an N-1 contingency. The WECC/NERC voltage performance criteria is formulated as constraints.

Chapter 3 presents the proposed approach used in this work to perform the heuristic linear programming. The role of voltage trajectory sensitivities in the optimization problem is to find the optimal location, the role of the heuristic linear programming is to determine the optimal var injection values and the role of Voronoi diagram is to tackle the non-convex feasible solution area.

Chapter 4 gives a demonstration of the voltage trajectory sensitivity index and heuristic linear dynamic optimization methods on a WECC 9-bus system and IEEE 39-bus system. Simulation results of voltage trajectories, optimal var injection values and search path for different operating conditions are presented. Also, Voronoi diagram tackle the feasible solution area of 2-dimension and 3-dimension in 9-bus system and 39-bus system respectively and the result is confirmed to be global optimal.

Chapter 5 summarizes the conclusions of the thesis, and proposes the future work.

Chapter 2 Formulation of the Problem

This chapter presents the formulation of the dynamic reactive power resource allocation problem considering the dynamic power system standard.

To address the fault-induced delayed voltage recovery (FIDVR) issues, power companies follow certain planning standards to manage dynamic var sources for the limitation of voltage dip/sag after a fault [12]. WECC/NERC gives the planning standards as shown in Fig. 2-1[13].

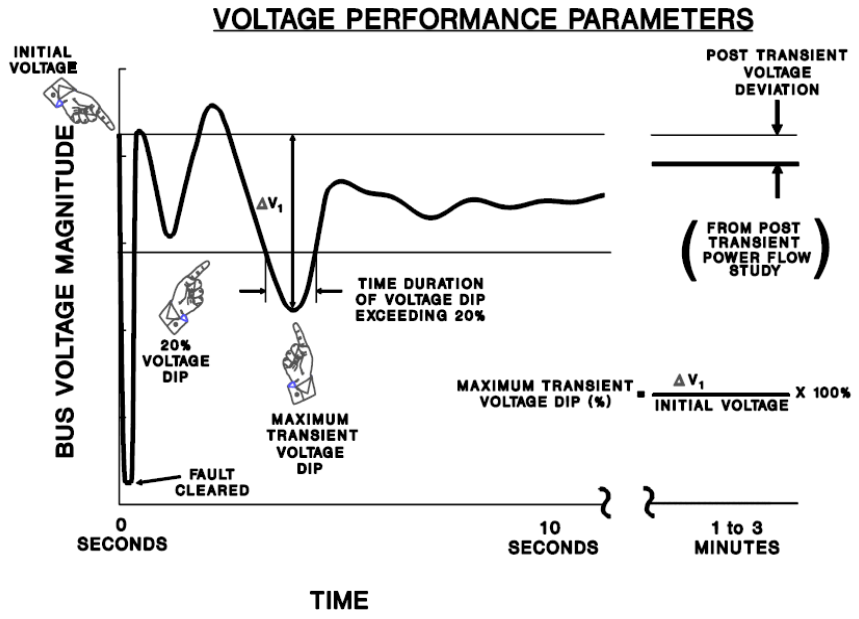

Figure 2-1.WECC/NERC Post-fault voltage performance criteria

The specific data of WECC/NERC standard for N-1 and N-2 criteria are listed in Table 1. For example, N-1 disturbance in one system shall not cause a transient voltage dip that is greater than 20% in anther system for more than 20 cycles at load buses, namely 40 steps with half cycle simulation step in 60Hz system. If the post transit voltage

deviations are less than the values in Table 1, it will result in voltage instability. The disturbance originated system and its affected neighboring system should cooperate manually to resolve the problem. WECC/NERC voltage criteria can be applied to either a system with all elements in service, or a system with one element removed and the system adjusted.

Table 1. WECC/NERC voltage criteria

NERC and WECC categories	**Transient voltage standard**	**Post transient voltage deviation standard**
N-1	Not to exceed 25% at load bus or 30% at non-load buses Not to exceed 20% at more than 20 cycles at load bus	Not to exceed 5% at any bus
N-2	Not to exceed 30% at any bus Not to exceed 20% for more than 20 cycles at load buses	Not to exceed 10% at any bus

2.1 Objective function

The objective function of the dynamic var allocation problem is formulated as:

Minimize

$$f = \sum c_i Q_i \tag{2-1}$$

where Q_i is the dynamic var injected at candidate bus i, c_i is the general cost coefficient associated with Q_i, e.g. the cost per Mvar of a SVC which can be either installation cost, maintenance cost or operation cost.

2.2 System Constraints

Without losing generality, this thesis considers typical voltage criteria according to WECC/NERC planning standards and formulated the standard as shown in Fig. 2-2. The post-fault transient voltage performance is expected to meet criteria such as:

1. The post-fault voltage deviation at a bus relative to its pre-fault initial voltage should not exceed D_1%.
2. The duration of a post-fault voltage dip or overshoot >D_2% should not exceed L cycles.
3. The post transient (starting from t_s seconds) voltage deviation at a bus should not exceed D_3%.

This thesis considers N-1 typical parameters in the criteria:

- D_1=25 (%) for load buses and 30(%) for generator buses
- D_2=20 (%) and L=20 (cycles) for load buses
- t_s=3 (seconds) after the fault clearing time (denoted by t_{cl}) and D_3=5 (%)

N-2 typical parameters are also taken into account in the criteria:

- D_1= 30(%) for any bus in the system
- D_2=20 (%) and L=40 (cycles) for load buses
- t_s=3 (seconds) after the fault clearing time (denoted by t_{cl}) and D_3=10 (%)

Fig. 2-2 illustrates the general formulation of criteria for a load bus.

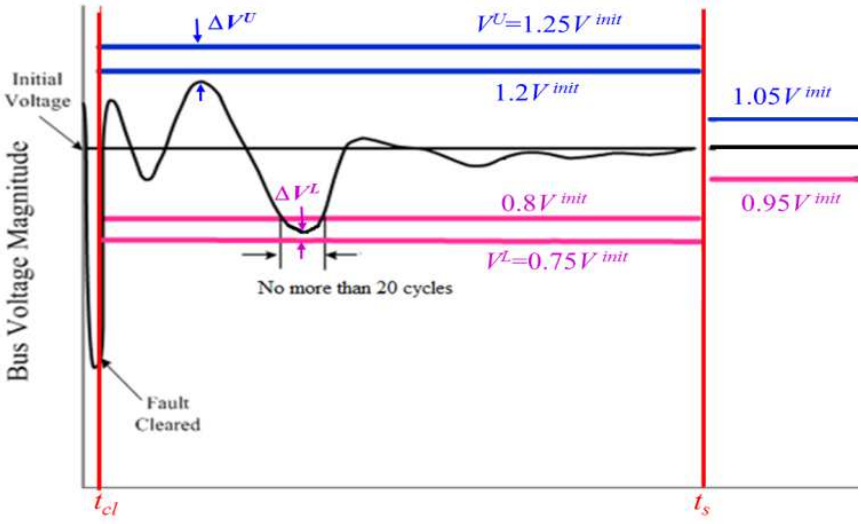

Figure 2-2. Post-fault voltage performance criteria.

Assume the system has *N* buses. Define the percentage voltage deviation of a bus j at time t:

$$R_j = \left|\frac{V_j(t) - V_j^{init}}{V_j^{init}}\right| \times 100\%, \forall j \in 1 \sim N \qquad (2\text{-}2)$$

where $V_j(t)$ is the j th bus voltage simulation result, V_j^{init} is the pre-fault initial voltage magnitude.

2.3 Combination

According to the aforementioned analysis, the optimal allocation problem for dynamic var sources (taking SVC as an example) can be formulated as follows for N-1 contingency.

Minimize

$$f = \sum_{i \in I_Q} c_i Q_i \tag{2-3}$$

All of subject to

$$Q_i^L \le Q_i \le Q_i^U, \forall i \in I_Q \tag{2-4}$$

$$R_j \le 25\%, t_{cl} \le t < t_s, \forall j \in I_L \tag{2-5}$$

$$R_j \le 30\%, t_{cl} \le t < t_s, \forall j \in I_G \tag{2-6}$$

$$R_j \le 5\%, t \ge t_s, \forall j \in 1{\sim}N \tag{2-7}$$

$$Duration_{R_j \ge 20\%} < 20\ cycles, t_{cl} \le t < t_s, \forall j \in I_L \tag{2-8}$$

$$\dot{x} = f(x, y, Q) \tag{2-9}$$

where Q_i^L and Q_i^U are the lower and upper limits of Q_i, I_L and I_G are respectively the sets of load and generator buses, (2-9) represents the differential and algebraic equations (DAEs) on power system dynamics, *x* and *y* are vectors of differential variables and algebraic variables, and *Q* is the vector of Q_i.

With the post-fault voltage trajectories from time-domain simulation, the above constraint in (2-8) may be checked for each simulation time step Δ*t*. For example, if Δ*t*= 0.005s, 20 cycles in 60 Hz systems correspond to around 67 time steps or if Δ*t*= 0.00833s, 20 cycles in 60 Hz systems correspond to about 40 time steps. Then, the

constraint requires that the duration of a >20% voltage deviation should not be more than 67 steps or 40 steps respectively.

The region of all solutions for the above optimization problem (2-3) ~ (2-9) may be non-convex, and that optimization is coupled with solving DAEs for post-fault power system trajectories. Therefore, it would be complicated to directly solve the problem. For example, for an exhaustive searching method, the post-fault voltage response should be solved with every potential combination of values of Q_i's and then voltage criteria can be checked so as to judge whether it is a feasible solution or not. The next chapter of this thesis proposes an efficient approach to cope with the problem as well as a valid visualization tool as an implementation to tackle the non-convex feasible solution area.

Chapter 3 Proposed Approach

3.1 Identification of the Most Critical Contingency

Assume the result of the new approach can satisfy the most critical contingency, it will enable other contingencies in the system meet the standard. Hence, to identify the most contingency in the system is important. Contingency severity analysis based on the steady state cannot capture the whole critical information of power system such as the transit voltage dip or overshoot at one bus or duration when the bus was below the acceptable limit. To effectively measure these factors, voltage performance indices based on WECC/NERC N-1 contingency criteria are discussed. Power system abnormal state during transit period and post fault period can be measured by voltage dip and overshoot at buses. Severity index, SI, is used to reflect the rigidity of the contingency including the lower limit violation and upper limit violation and calculated at each time simulation step. This thesis takes the severity index of N-1 contingency as example.

$$SI_{ij}{}^{t} = \begin{cases} 1, R_j \geq 25\%, t_{cl} \leq t < t_s, \forall j \in I_L \\ 1, R_j \geq 30\%, t_{cl} \leq t < t_s, \forall j \in I_G \\ 1,\ R_j \geq 5\%, t \geq t_s, \forall j \in 1{\sim}N \\ 0, otherwise \end{cases} \tag{3-1}$$

Then the average severity of one N-1contingency in the system is expressed as

$$SI_i = \frac{1}{T}\sum_{t=1}^{T}\left(\frac{1}{N}\sum_{j=1}^{N} SI_{ij}{}^{t}\right) \tag{3-2}$$

where T is the total simulation step. SI_i can be estimated for every N-1 contingency in the system and the contingencies with larger values are taking as severer N-1 contingency in the system. The N-1 contingency with largest SI_i is selected as the

most critical contingency in the system which will then be used to determine the locations of dynamic var sources and optimize the size of reactive var sources.

3.2 Determination of the Locations of Dynamic Var Sources

For the most severe contingency, some candidate buses (i.e., I_Q) are selected among all N buses in the system. The candidate buses may be those where var injection can cause more sensitive improvements on the overall post-fault voltage level. For instance, the method based on a post-fault trajectory sensitivity index in [2] may be applied. Another similar index is the Voltage Sensitivity Index (VSI) which is defined below. A small amount of dynamic var q_i is injected at bus i, which can be simulated by adding a SVC of size q_i. Assume that the simulation time step is Δt, the total simulation period is $T \times \Delta t$, and the var injection changes the voltage at bus j from $V_j^{old,t}$ to $V_j^{new,t}$ at time step t from time-domain simulation results. VSI is calculated by (3-3) for each bus j at certain time step. For simplicity, this thesis considers VSI as the maximum voltage recovery sensitivity index as in (3-4) for each bus j over the simulation period.

$$VSI_{ij}{}^{t} = V_j^{new,t} - V_j^{old,t}/q_i\,, \forall\ t = 1{\sim}T \tag{3-3}$$

$$VSI_{ij} = \max[V_j^{new,t} - V_j^{old,t}, t = 1{\sim}T]/q_i \tag{3-4}$$

Then the average recovery sensitivity for the system about the var injection at bus i is given by

$$VSI_i = \frac{1}{N}\sum_{j=1}^{N} VSI_{ij} \tag{3-5}$$

VSI_i can be estimated for every bus and the buses with higher values are selected as the candidate buses to add dynamic var sources.

3.3 Optimization of the Sizes of Dynamic Var Sources

Assume that there are n candidate buses, i.e., $|I_Q|=n$. The heuristic approach proposed in this thesis conducts the following steps to determine the sizes of the dynamic var sources (taking SVCs as an example), i.e., $Q_1 \sim Q_n$:

1. In the n-dimensional space of $Q_1 \sim Q_n$, the initial guesses (denoted by $Q_1^0 \sim Q_n^0$) are selected at a feasible solution to satisfy all post-fault voltage criteria or at a solution without violating voltage criterion as in (2-8). Let $k=0$
2. Time-domain simulation on the most severe contingency is conducted with SVC models of sizes $Q_1^k \sim Q_n^k$ added to the candidate buses. Then, a small amount q_i is added, e.g., $Q_i^k/10$, to each candidate bus and re-simulate the contingency. VSI_{ij} is calculated by using the voltage responses with or without q_i according to (3-4).
3. Use VSI_{ij} as the heuristic information to optimize the amount of update ΔQ_i^k by solving a LP problem. Then, let $Q_i^{k+1} = Q_i^k + \Delta Q_i^k$
4. Iterate Steps 2 and 3 until one of the following stopping criteria is met:
   i. If all $|\Delta Q_i^k|$'s are smaller than an inaccuracy limit ε and the voltage responses with Q_i^{k+1} satisfy all voltage criteria, then let $Q_1 \sim Q_n = Q_1^{k+1} \sim Q_n^{k+1}$
   ii. If $k+1$ exceeds a preset maximum iteration number K (e.g. 10~20), let $Q_1 \sim Q_n$ take the results from the most recent iteration that does not cause any violation of voltage criteria

The second stopping criterion is to make sure the feasibility of the final solution in case that the LP solution after a number of iterations violates voltage criterion (2-8). If

then, the most recent feasible solution is provided, instead. Detailed algorithms in Step 3 to determine $\Delta Q_1^k \sim \Delta Q_n^k$ are presented below.

As illustrated in Fig. 2-2, define

$$\Delta V_j^{L,k} = \min[V_j^{k,t} - V_j^{L,t}, t = 1\sim T] \quad (3\text{-}6)$$

$$\Delta V_j^{U,k} = \min[V_j^{U,t} - V_j^{k,t}, t = 1\sim T] \quad (3\text{-}7)$$

where $V_j^{k,t}$ is the voltage of bus j at time step t, and $V_j^{L,t}$ =0.75V_j^{init} if $t < t_s$; otherwise $V_j^{L,t}$=0.95V_j^{init}. And $V_j^{U,t}$ =1.25V_j^{init} if $t < t_s$ or 1.05V_j^{init}, otherwise. The magnitudes of $\Delta V_j^{L,k}$ and $\Delta V_j^{U,k}$are actually the closest distances from the voltage trajectory to the two limits. $\Delta V_j^{L,k}$ ($\Delta V_j^{U,k}$) is positive if the trajectory is above (below) the limit, or negative, otherwise.

Then the following LP problem is solved to determine $\Delta Q_1^k \sim \Delta Q_n^k$.

Minimize

$$f = \sum_{i=1}^{n} c_i {Q_i}^{k+1} \quad (3\text{-}8)$$

Subject to

$$Q_i^{k+1} = Q_i^k + \Delta Q_i^k, \forall\, i = 1\sim n \quad (3\text{-}9)$$

$${Q_i}^L \le Q_i^{k+1} \le {Q_i}^U, \forall\, i = 1\sim n \quad (3\text{-}10)$$

$$V_j^{L,t} \le V_j^{k,t} + \sum_{i=1}^{n} {VSI_{ij}}^t {\Delta Q_i}^{k,t} \le V_j^{U,t},\ t = 1\sim T,\ \forall j \in 1\sim N \quad (3\text{-}11)$$

(3-11) can be written as

$$V_j^{L,t} - V_j^{k,t} \le \sum_{i=1}^{n} {VSI_{ij}}^t {\Delta Q_i}^{k,t} \le V_j^{U,t} - V_j^{k,t}, t = 1\sim T, \forall j \in 1\sim N \quad (3\text{-}12)$$

Similarly as the ${VSI_{ij}}^t$ and VSI_{ij}, (3-12) can be simplified in following way of just considering the minimum distance between voltage and voltage limits over the whole simulation.

$$\min(V_j^L - V_j^k) \leq \sum_{i=1}^n VSI_{ij}{\Delta Q_i}^k \leq \min(V_j^U - V_j^k), \forall j \in 1{\sim}N \tag{3-13}$$

For the first two parts of (3-13), it can transfer to the following format:

$$\sum_{i=1}^n VSI_{ij}{\Delta Q_i}^k \geq \min(V_j^L - V_j^k), \forall j \in 1{\sim}N \tag{3-14}$$

For the right part of the inequality, it equals to the $-\Delta V_j^{L,k}$ based on the (3-6), thus (3-14) can be written as:

$$\sum_{i=1}^n VSI_{ij}{\Delta Q_i}^k \geq -\Delta V_j^{L,k}, \forall j \in 1{\sim}N \tag{3-15}$$

Yielding

$$-\sum_{i=1}^n VSI_{ij}{\Delta Q_i}^k \leq \Delta V_j^{L,k}, \forall j \in 1{\sim}N \tag{3-16}$$

As for the second two parts of the (3-13), it can be simplified as (3-17) based on (3-7).

$$\sum_{i=1}^n VSI_{ij}{\Delta Q_i}^k \leq \Delta V_j^{U,k}, \forall j \in 1{\sim}N \tag{3-17}$$

Since the system is very non-linear system, the VSI_{ij} may not be as linear as adding small amount of var. In order to speed up the searching, (3-16) and (3-17) can be multiply acceleration factors as shown in (3-18) and (3-19) respectively, which is 1 as default value.

$$-\sum_{i=1}^n \alpha_{i,j} VSI_{ij}{\Delta Q_i}^k \leq \Delta V_j^{L,k}, \forall j \in 1{\sim}N \tag{3-18}$$

$$\sum_{i=1}^n \beta_{ij} VSI_{ij}{\Delta Q_i}^k \leq \Delta V_j^{U,k}, \forall j \in 1{\sim}N \tag{3-19}$$

The above LP problem is to approximately find the minimum var requirement for the improvement of the post-fault voltage performance by pushing the post-fault voltage trajectories as close to the lower voltage limit as possible. $\Delta Q_1^k \sim \Delta Q_n^k$ are solved to update $Q_1^k \sim Q_n^k$ for the next iteration. The constraints (3-18) and (3-19) indicate that the voltage response is expected to stay within the two limits and approach the lower limit to save the total cost.

3.4 Implementation of the Approach

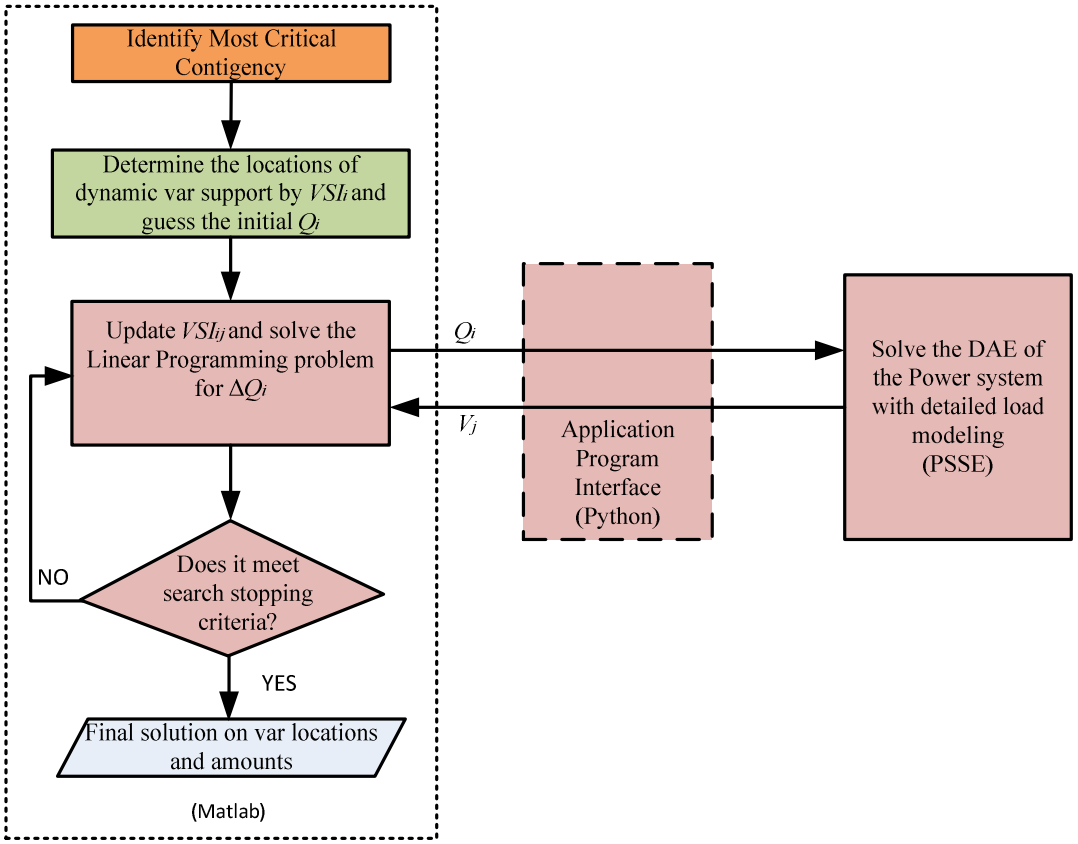

Figure 3-1. Flow chart for implementing the proposed approach.

Fig. 3-1 illustrates the implementation diagram of the new approach. The approach interfaces the LP algorithm (MATLAB code) with the power system dynamics simulator (i.e., PSS/E) via Python. PSS/E solves the DAEs in (2-9) to simulate the post-fault voltage responses for any given var injection strategy. The results are fed back to the LP algorithm for voltage criteria check and VSI_{ij}, $\Delta V_j^{L,k}$and $\Delta V_j^{U,k}$ calculation. Induction motor loads and SVCs are needed to be modeled in PSS/E simulations.

3.5 Tackling the feasible solution area

Voronoi diagram is a widely applied technique of computational geometry. Its fundamental framework is first based on the certain number of sample points calculated from the above method within design space which also means the boundary of the dynamic var. Second, an approximated objective function is generated according to the information given from the analysis result at sample points. Third, an optimal solution is estimated with above optimization algorithm over the approximated function instead of direct analysis. In this thesis, Voronoi diagram is applied for the optimal placement of new sample and barycentric interpolation [14-17] is used to estimate the tentative optimal objective function.

3.5.1 Definition and basic properties of Voronoi diagram

Denote the Euclidean distance between two points p and q by $dis(p,q)$. In the plane, we have $dis(p,q) = \sqrt{(p_x - q_x)^2 + (p_y - q_y)^2}$. Let $P = \{p_1,\ p_2, \cdots p_{10}\}$ be a set of n distinct points in the two dimension space shown as in Fig. 3-2(a). Perpendicular bisectors are drawn for each pair of points shown as triangular edge in Fig. 3-2(b). This

results in a set of polygons which will be polyhedra in the higher dimensional space. These polygons as Voronoi regions are denoted diagram of P by Vor(P). One for each site in P, with the property that a point q lies in the cell corresponding to a site p_i if and only if $dis(q, p_i) < dis(q, p_j)$ for each $p_j \in P$ with $j \neq i$. All of the intersection points q_1, q_2,..., q_9,..., are named Voronoi points.

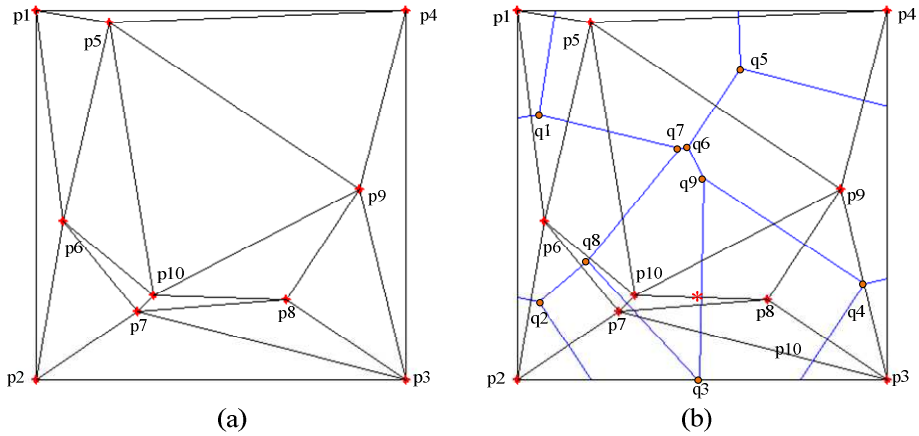

Figure 3-2. Voronoi diagram.

3.5.2 Barycentric interpolation

Barycentric interpolation is a variant of Lagrange polynomial interpolation which is also known as area coordinates or areal coordinates. Barycentric interpolation is useful especially in engineering applications involving triangular subdomains. Taking the triangle which composited by p_5, p_9, p_{10} as an example, its three vertices have three objective values as shown in Fig. 3-3. Each point located inside this triangle can be written as a unique convex combination of the three vertices. In other words, for each point there is a unique sequence of three numbers. If we want to estimate the objective

value of q_9, there is a unique sequence of three numbers, $\alpha_1, \alpha_2, \alpha_3 \geq 0$ such that $\alpha_1 + \alpha_2 + \alpha_3 = 1$ and $q_9 = \alpha_1 p_5 + \alpha_2 p_{10} + \alpha_3 p_9$. The three numbers $\alpha_1, \alpha_2, \alpha_3$ indicate the barycentric or area coordinates of the point q_9 with respect to the triangle. Every point inside the triangle of p_5, p_9, p_{10} is uniquely defined by any two of the barycentric coordinates.

Where,

$$\alpha_1 = percent\ green\ area = \frac{area\ of\ green\ triangle}{total\ area} = \frac{A1}{A1 + A2 + A3}$$

$$\alpha_2 = percent\ blue\ area = \frac{area\ of\ blue\ triangle}{total\ area} = \frac{A2}{A1 + A2 + A3}$$

$$\alpha_3 = percent\ orange\ area = \frac{area\ of\ orange\ triangle}{total\ area} = \frac{A3}{A1 + A2 + A3}$$

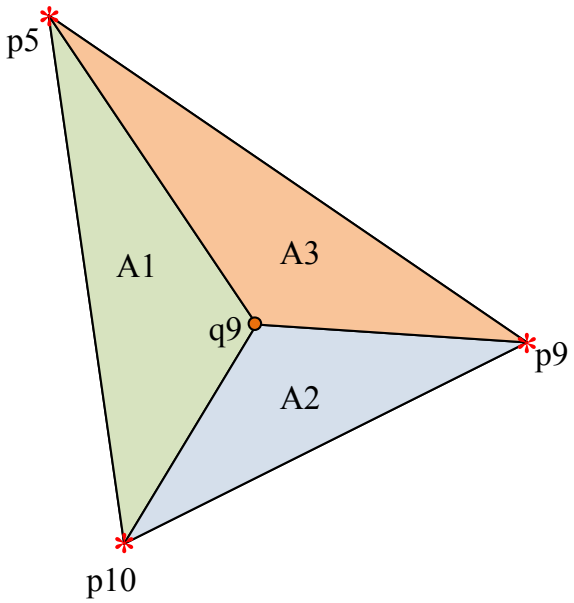

Figure 3-3. Barycentric interpolation.

3.5.3 Addition of new sample

In order to improve global approximation fidelity, selecting new samples besides the samples tried in linear algorithm is significant.

1. Selection of candidate region and adjustment of a new sample point for the optimal objective function.

   The triangle where the tentative optimal solution is obtained is considered as the most effective area. A new sample point is chosen based on the minimum objective function from the barycentric interpolation.

2. Selection of new sample point for global fidelity.

   For this purpose, a region where existing sample points are depopulated must be effective. Under the terminology of Voronoi diagram, each Voronoi point is the most far point from its surrounding sample points. A new sample point is chosen based on the largest $dis(p_i, q_i)$ and q_i is the candidate new second point.

3. Selection of new sample point connecting the second and first sample points.

   Adding new samples at the above two types of point, the density of samples around the tentative optimal and around the most depopulated one become quite different. A new sample point is chosen in the middle of the interconnection of the above two samples.

3.5.4 Overall algorithm of area tackle

The overall algorithm for tackling the area is configured into following steps:

1. Based on certain number of initial sample points from the linear searching path and execute system analysis at those points.
2. Establish or update the Voronoi diagram and estimate the objective function by barycentric interpolation.
3. Find a tentative solution by solving an approximated objective function.
4. If a solution has enough fidelity or if the cost exceeds the limit, terminate the overall procedure.
5. Determine new sample points, and execute system analysis there.
6. go to Step 2

Chapter 4 Case Studies

The proposed new approach is tested by case studies on the WECC 9-bus system and IEEE 39-bus system. The studies apply the CLODBL load model and CSVGN5 SVC model (see [18] for details) to simulate the phenomena of FIDVR and dynamic var supporting.

4.1 Setup for simulation

The CLODBL load model is used for planning and operation studies in the power system in PSS/E. This model is consisted of induction motors, lighting and other types of equipment shown as Fig. 4-1. It is intended to use in situations where it is desirable to represent loads at the dynamic level. The model allows the user to specify a minimum amount of data stating the general character of the composite load. It uses this data internally to establish the relative sizes of motors modeled in dynamic detail. In this thesis, all the parameters of composite load are listed in the Table 2.

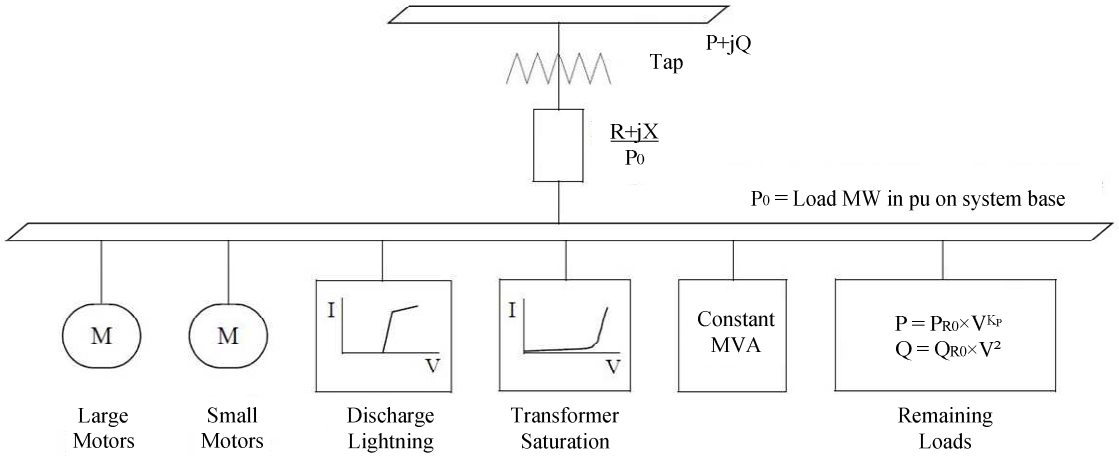

Figure 4-1. Composite load model.

Table 2. Parameters for composite load model

Parameters	Value
PC_LM,% large motor	25
PC_SM,% small motor	25
PC_TX,% transformer exciting current	1
PC_DL,% discharge lighting	20
PC_CP,% constant power	5
Kp,% of remaining	3
R, branch resistance(pu load MW base)	0
X, branch reactance(pu load MW base)	0.1

CSVGN5 SVC model is static var system model that were written for a corresponding model in the WECC stability program in PSS/E. It is represented as generator in the power flow simulation. In the dynamic simulation, CSVGN5 has fast override capability which is activated when the voltage error exceeds a threshold value. It does not to separate the equipment to identify capacitor banks and reactors. The output of CSVGN5 is equal to B_{max} and the thyristor controlled reactor is shut off. If B_{max} is positive then the capacitor banks are equal to B_{max} times the MVA rating in the power flow from the generator setup. If B_{max} is negative, then the equipment is assumed to consist of just reactor.

In the case studies, we assume all c_i=1, i.e. all buses have identical costs for SVCs. In this case the objective is actually to minimize the total amount of dynamic var supports to meet the voltage criteria. The total post-fault simulation time is 5s and the post transient criterion is checked after the first 3 seconds transient period. No upper limit is set for the size of dynamic var supports. For both case studies, let q_i= 5Mvar, the maximum iteration number K=10, and inaccuracy limit ε=1Mvar.

4.2 9-bus system

The 9-bus system has 3 generators, 3 transformer, 3 loads, and 5 transmission lines, as shown in Fig. 4-2. According to contingency analysis, a three-phase fault on bus 7, which is cleared by opening the line between buses 7-5 after 5 cycles, is identified as the most severe N-1 contingency. The delayed voltage recovery phenomenon is simulated as shown in Fig. 4-3. 5 out of 9 bus voltages violate the voltage criteria.

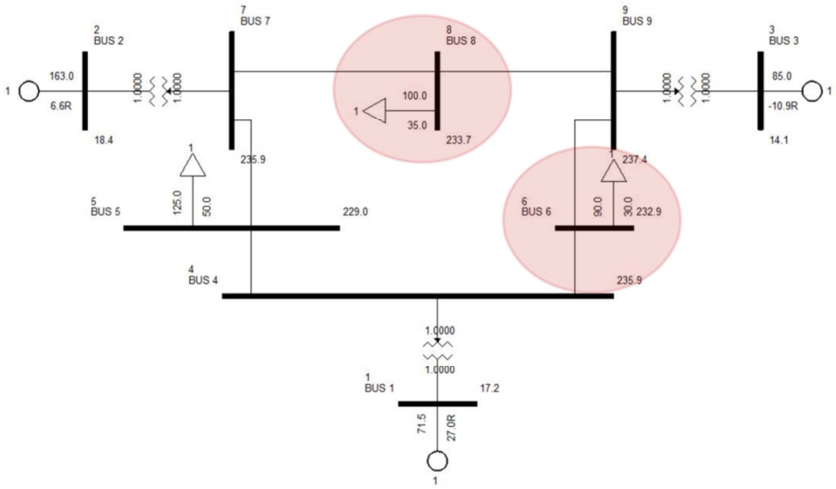

Figure 4-2. 9-bus system with the most severe N-1 contingency and two candidate buses for dynamic var supports.

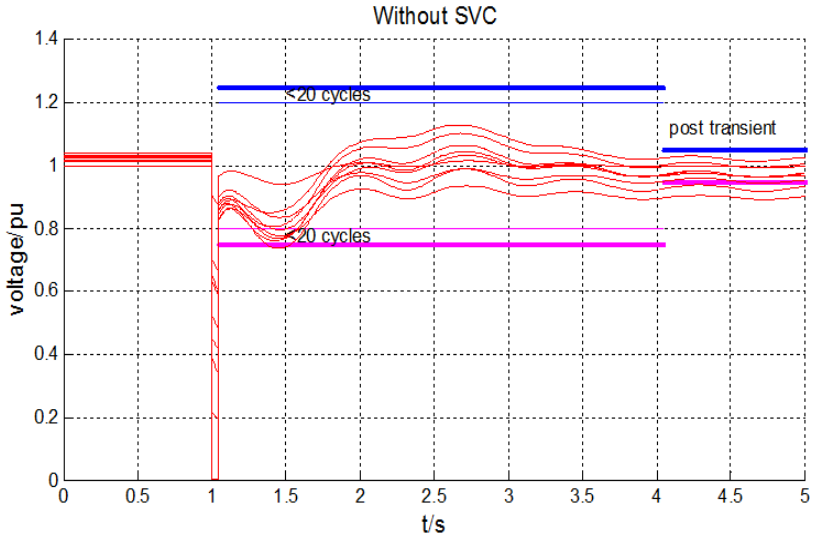

Figure 4-3. Bus voltage responses of the 9-bus system.

At Buses 6 and 8, the overall VSI is higher than that at other buses as listed. So they are selected as two candidate buses to install SVCs. Assume the sizes of the two SVCs are larger than 1Mvar. The initial guesses of Q_6 and Q_8 are set at 30Mvar and 50Mvar, respectively. As shown in Fig. 4-4, after 4 iterations the proposed approach converges to a solution: Q_6=56Mvar and Q_8=1Mvar.

To investigate the global optimality of this solution, an exhaustive search is conducted to estimate the entire region of feasible solutions as shown by the gray region in Fig. 4-4. It is confirmed that the obtained solution is the global optimum although the solution region is non-convex. For this case, the initial guesses do not correspond to a feasible solution but the first iteration jumps to a feasible solution. To test the voltage performance with the optimal var injections, time-domain simulation is conducted with

SVCs added to Buses 6 and 8 with the determined sizes. Fig. 4-5 shows that all trajectories meet the voltage criteria.

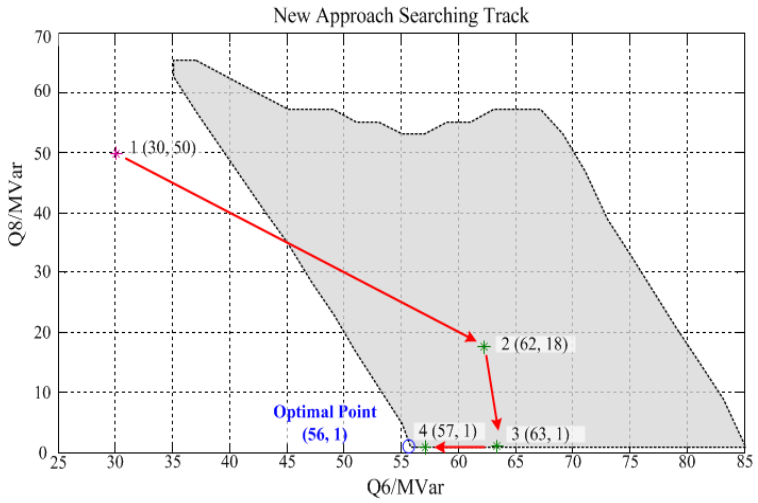

Figure 4-4. Searching path of the new approach for the 9-bus system.

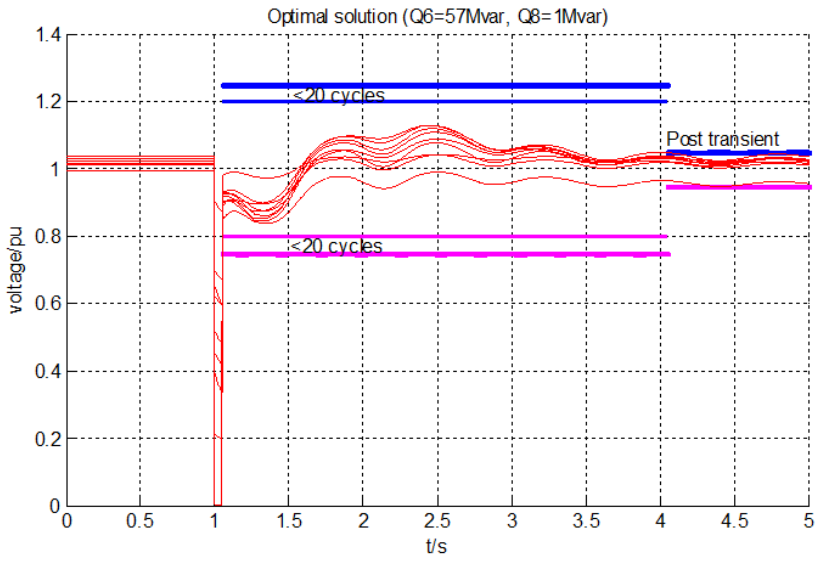

Figure 4-5. Post-fault voltage responses with optimized SVCs for the 9-bus system.

In Fig. 4-6, the non-convex feasible solution area is tackled by the Voronoi diagram which is bounded by the light blue color. The darker blue indicates the smaller objective function. From the diagram, it verifies the result from the heuristic linear programming is global optimal.

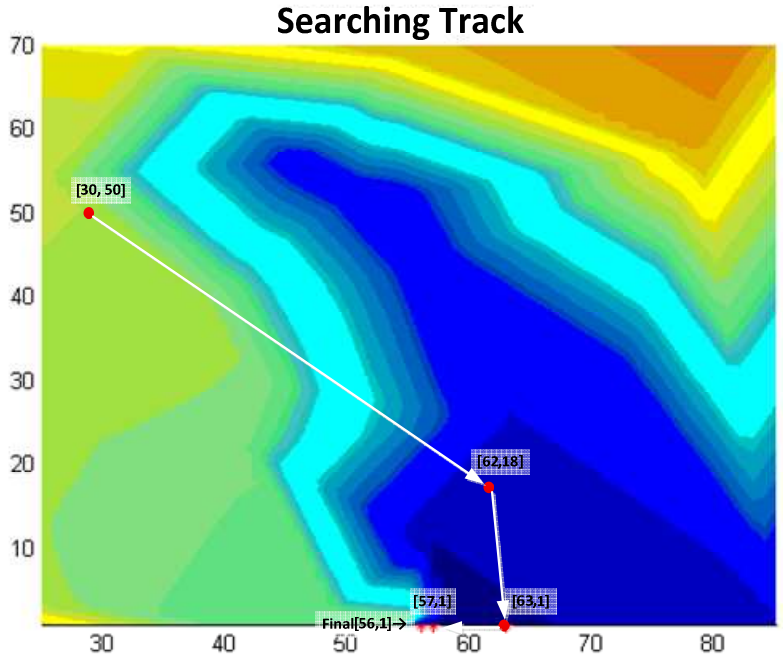

Figure 4-6. Feasible solution area of 2 dimesion seach space.

The approach in [7] is implemented with 0.005s time step to compare with the new approach. It is found that the two approaches give identical solutions. However, the new approach is about 10 times faster for this case using an Intel i5-3220M computer. The reason is because the new approach only handles a LP problem and it does not need to interface the optimization solver with power system simulator for each time step as the approach in [7] does.

4.3 IEEE 39-bus System

As shown in Fig. 4-7, the IEEE 39-bus system is also used to test the proposed approach. The most severe contingency is identified as a three phase fault on Bus 17 cleared by opening Lines 17-18 and 17-27 after 5 cycles. Post-fault voltage trajectories are shown in Fig. 4-8. Some buses violate the 25% voltage deviation limit at the beginning of the 3-second transient period or the 5% limit at the beginning of the post transient period.

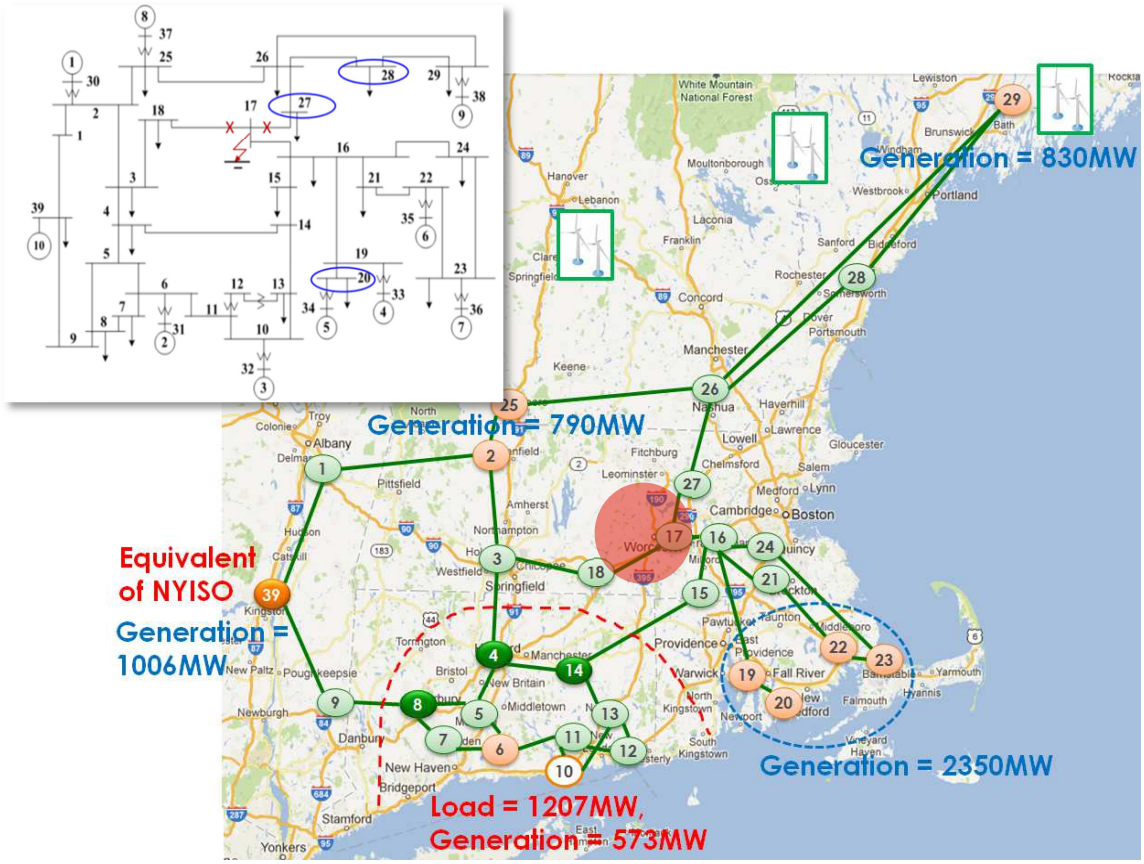

Figure 4-7. IEEE 39-bus system and the most severe N-2 contingency and three candidate buses for dynamic var supports.

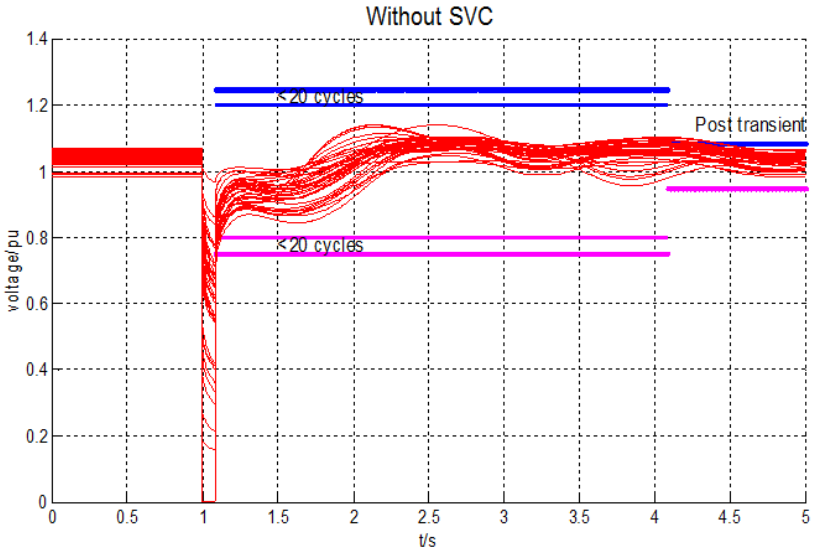

Figure 4-8. Post-fault voltage responses of the IEEE 39-bus system.

Assume that the sizes of SVCs are larger than 25Mvar and have no upper limits. The new approach is applied to find the optimal locations and sizes of SVCs to support the voltage recovery. First, buses 20, 27, and 28 are found to have the highest VSI values and thus selected to be candidate buses. The top 5 highest VSI buses are listed in Table 3.

Table 3. Top 5 highest VSI buses in 39-bus system

BUS NO.	VSI	Rank based VSI
28	0.0971	1
27	0.0297	2
20	0.0236	3
26	0.0229	4
21	0.0202	5

Then, conduct the heuristic searching algorithm to optimize Q_{20}, Q_{27} and Q_{28}. Select an initial point (280, 280, 280) in the space of Q_{20}, Q_{27} and Q_{28}. As shown in Fig. 4-9, after 4 iterations the optimal solution is found to be Q_{20}=326 Mvar and Q_{27}=Q_{28}=25 Mvar. This solution is verified to be the global optimum by an exhaustive search in the 3-dimensional space. Fig. 4-9 also shows the boundary of feasible solutions by the gray plane.

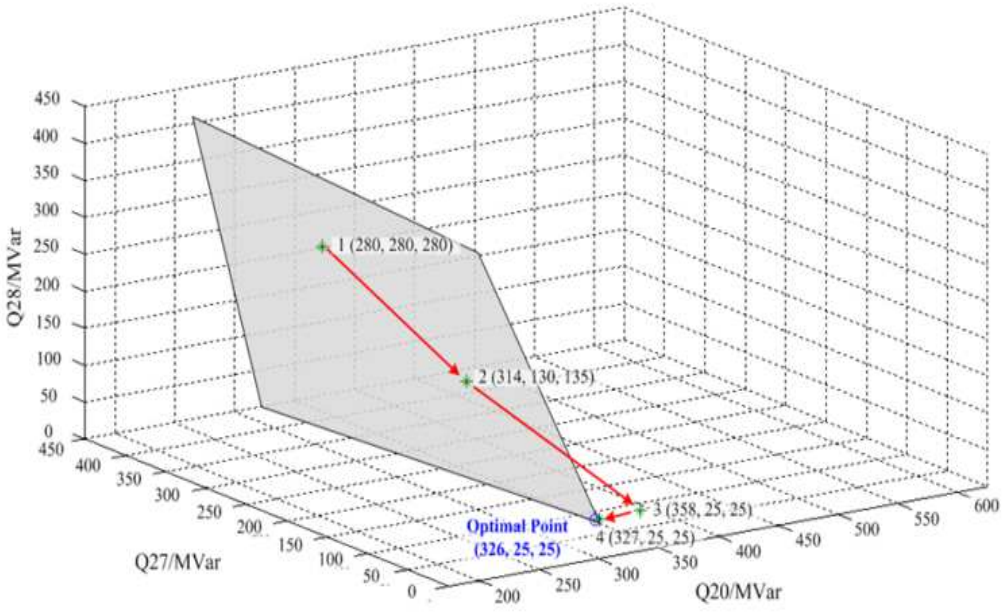

Figure 4-9. Searching path of the new approach for the IEEE 39-bus system.

The optimal solution is tested by time-domain simulation with SVCs of the optimized sizes added at the three candidate buses. Fig. 4-10 and Fig. 4-11 show that all post-fault voltage trajectories meet the voltage criteria while in Fig. 4-11 the solution is not optimal which costs more to install var sources.

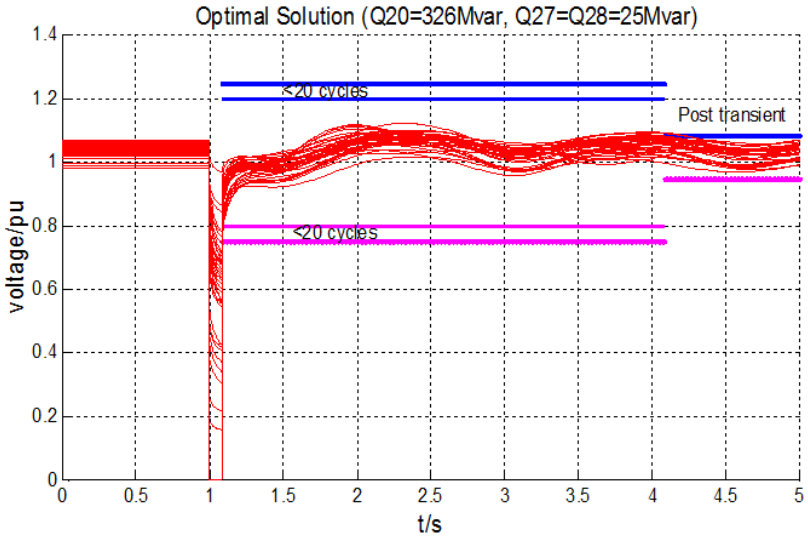

Figure 4-10. Post-fault voltage responses with optimized SVCs of the IEEE 39-bus system.

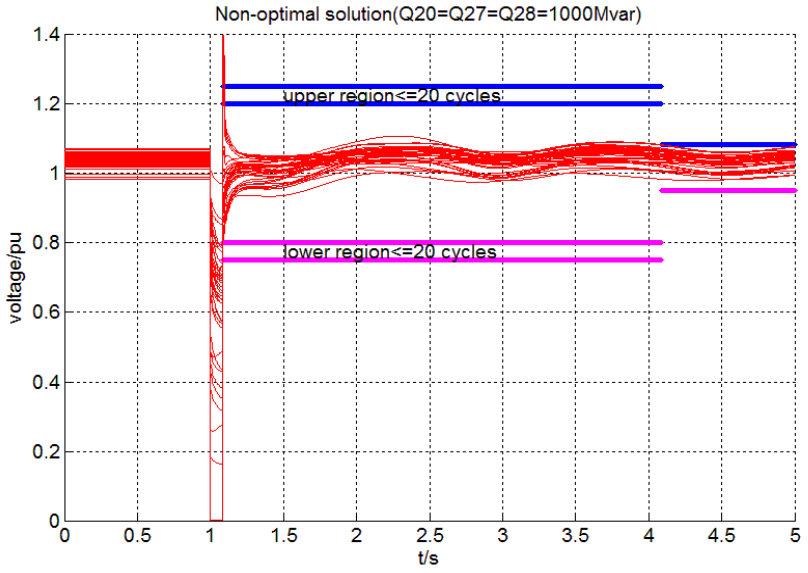

Figure 4-11. Post-fault voltage responses with over-compensated SVCs of the IEEE 39-bus system.

Also, Voronoi diagram is implemented in the IEEE-39 bus system to plot the contour map. In order to view the plot clearly, the contour map is projected into 2-D dimension. From Fig. 4-12, the feasible solution area of the system is bounded by the light blue color within which darker color indicates smaller objective function. The optimal solution is located on the right front corner. We can conclude that the result from the new approach is global optimal.

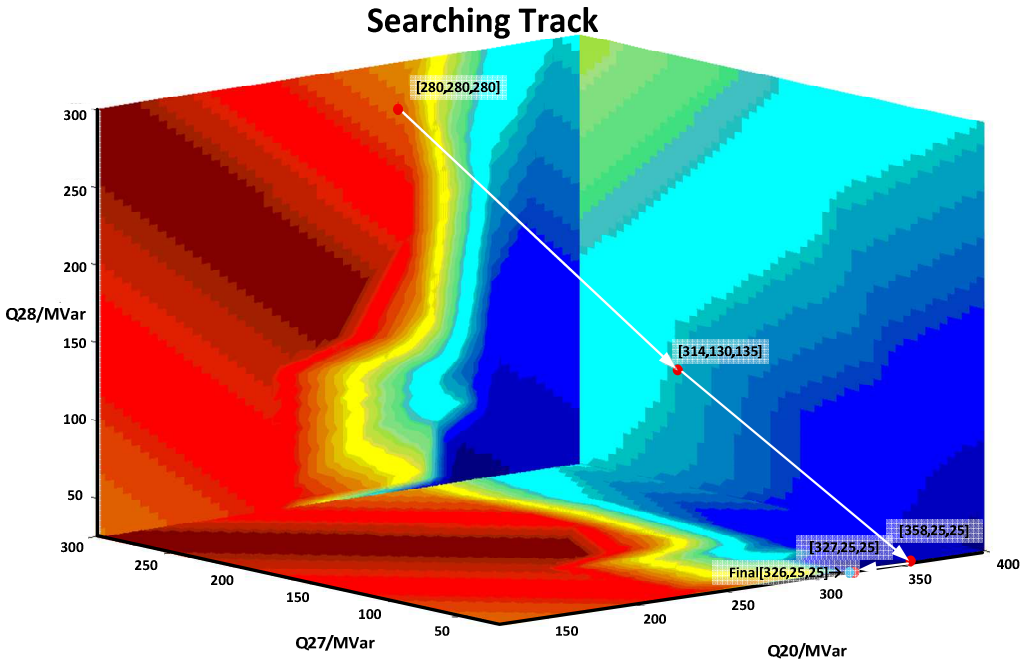

Figure 4-12. Projected contour map into 2-D.

Chapter 5 Conclusion and Future Work

5.1 Conclusion

All of the work in this thesis is done to address the FIDVR issue in the power system which may cause voltage collapse or even cascading failure. First, a severe sensitivity index is to identify the most critical contingency in the system. Based on that, a voltage sensitivity index is to rank buses by sensitivity for installation of dynamic var sources. Then, a new approach is proposed to optimal the sizes of dynamic var sources. Finally, the Voronoi diagram is implemented to tackle the non-convex feasible solution area of the nonlinear problem for verifying the result. The new approach was validated on WECC 9-bus system and IEEE 39-bus system.

Also, the new approach was benchmarked with the approach in reference [7] and was proved to be more efficient thanks to its heuristic searching algorithm.

5.2 Future work

For more practical and efficient optimization of dynamic var sources to address FIDVR issues, the following work should be considered in future:

1) Improve the approach to address multiple contingencies rather than the most severe one.
2) Test the new approach on more realistic larger power system models, e.g. CURENT's NPCC 140-bus testbed system and an eastern interconnection model.

3) Consider optimization with other types of dynamic var sources such as wind turbines, HVDC and power electronics-interfaced devices.

List of References

[1]. P. Kundur, “Power system stability and control, ” McGraw Hill, Newyork, 1994.

[2]. B. Sapkota and V. Vittal, “Dynamic var planning in a large power system using trajectory sensitivities,” *IEEE Trans. Power Syst.*, vol. 25, no. 1, pp. 461-469, Feb. 2010.

[3]. P. Pourbeik, R. J. Koessler, W. Quaintance, and W. Wong, “Performing comprehensive voltage stability studies for the determination of optimal location, size and type of reactive compensation,” *IEEE PES General Meeting. 2006*.

[4]. V.S. Kolluri, and S. Mandal, “Determining reactive power requirements in the southern part of the energy system for improving voltage security-A case study”, *IEEE PSCE*, 2006.

[5]. A. P. S. Meliopoulos, G. Cokkinides, and G. Stefopoulos, “Voltage stability and voltage recovery: load dynamics and dynamic var sources”, *IEEE PES General Meeting*, Oct. 2006.

[6]. A. Tiwari and V. Ajjarapu, “Optimal allocation of dynamic var support using mixed integer dynamic optimization”, *IEEE Trans. Power Syst.*, vol. 26, no. 1, pp. 305-314, Feb. 2011.

[7]. M. Paramasivam, et al, , “Dynamic optimization based reactive power planning to mitigate slow voltage recovery and short term voltage instability”, *IEEE Trans. Power Syst.*, vol. 28, no. 4, pp. 3865-3873, Nov. 2013.

[8]. M. G. O. Cheong, M. Kreveld, and M. Overmars, “Computational Geometry: algorithms and applications (3rd ed.),” Springer-Verlag, New York, 2008.

[9]. D. Yan, G. Bao, X. Zhang and P. Wonka, “Low-resolution remeshing using the localizaed restricted Voronoi diagram”, *IEEE Trans. Visualization and Computer Graphics* vol. 20, no. 10, pp. 1418-1427, Oct. 2014.

[10]. N. Hirokawa, K. Fujita, and T. Iwase, “Voronoi diagram based blending of quadratic response surfaces for cumulative global optimization”, *Proceedings 9th AIAA/ISSMO Symposium on Multi-Disciplinary Analysis and Optimization*, Paper number AIAA-2002-5460.

[11]. W. Huang, K. Sun, J. Qi, and Yan Xu, “A New Approach to Optimization of Dynamic Reactive Power Sources Addressing FIDVR Issues”, *IEEE PES General Meeting*, Jul. 2014.

[12]. D. J. Shoup, J. J. Paserba, and C. W. Taylor, “A survey of current practices for transient voltage dip/sag criteria related to power system stability,” *IEEE PES PSCE*. Oct, 2004.

[13]. NERC/WECC Planning Standards, WECC, Apr., 2003.

[14]. J. Berrut and L. N. Trefethen, “Barycentric Lagrange interpolation,” *Scocity for Industrial and Applied Mathematics*, vol. 46, no. 3, pp. 501-517, 2004.

[15]. J. Berrut and H. D. Mittelmann, “Matrices for the direct determination of the barycentric weights of rational interpolation,” *Journal of Computational and Applied Mathematics*, 78 pp. 355-370, 1997.

[16]. A. A. Ungar, “Hyperbolic barycentric coordinates,” *The Australian Journal of Mathematical Analysis and Applications*, vol. 6, issue. 1, art. 18, pp. 1-35, 2009.

[17]. A. A. Ungar, “Barycentric calculus in Euclidean and hyperbolic geometry: a comparative introduction,” World Science, Singapore, 2010.

[18]. Siemens PTI Power Technologies Inc., PSS/E 33, Program Application Guide, vol. II, May 2011.

Vita

Weihong Huang was born in Taizhou, Zhejiang Province in China on Jan. 3rd, 1987. She received her B.S. degree in Electrical Engineering from Huazhong University of Science and Technology, Wuhan, China in 2009. She was a power grid dispatcher in the Yueqing Electric Power Bureau, Grid State Corporation of China, Wenzhou, China, from 2009 to 2012. She began her Ph.D. study on Power System in the University of Tennessee at Knoxville in 2013 spring. Her research interests are power system stability analysis, dynamics and operation control, and complex network optimization of reactive power management.